Effects of Synaptic Depression and Recovery on Synchronous Network Activity

Waldemar Swiercz, Krzysztof Cios,† Jennifer Hellier,* Audrey Yee,†† Kevin Staley**

Summary: The output of an artificial neural network of spiking neurons linked by glutamatergic synapses subject to use-dependent depression was compared with physiologic data obtained from rat hippocampal area CA3 *in vitro*. The authors evaluated how network burst initiation and termination was affected by activity-dependent depression and recovery under a variety of experimental conditions including neuronal membrane depolarization, altered glutamate release probability, the strength of synaptic inhibition, and long-term potentiation and long-term depression of recurrent glutamatergic synapses. The results of computational experiments agreed with the *in vitro* data and support the idea that synaptic properties, including activity-dependent depression and recovery, play important roles in the timing and duration of spontaneous bursts of network activity. This validated network model is useful for experiments that are not feasible *in vitro*, and makes possible the investigation of two-dimensional aspects of burst propagation and termination.

Key Words: Glutamate, Synaptic depression, Hippocampus, Network, Modeling, Computational.

(*J Clin Neurophysiol* 2007;24: 165–174)

The recurrent collateral synaptic connections in area CA3 of the hippocampus provide a powerful synchronizing mechanism such that when only one (Miles and Wong, 1983) or a few neurons fire synchronously, the rest of the population receives enough excitatory postsynaptic potentials (EPSPs) to fire also (Chamberlin et al., 1990). During these synchronous population events, CA3 pyramidal cells fire a series of action potentials during a 20 to 40 mV depolarizing membrane potential shift that begins and ends within a few milliseconds of the rest of the network (Traub and Wong, 1982). This discharge pattern corresponds to that seen *in vivo* during pathologic EEG sharp wave activity (Jefferys, 1998). The discharge lasts 50 to 250 milliseconds and is followed by several seconds of relative inactivity (quiescence) until the next discharge (Traub and Miles, 1991). The sudden transition to quiescence is unexpected: when GABAergic inhibition is blocked, the high degree of positive feedback should cause the CA3 network to discharge continuously (Mayr, 1970). Instead, a variety of manipulations that increase network excitability (Traub and Miles, 1991) result in periodic, synchronous discharges of all pyramidal cells in CA3; throughout the rest of this article, this is referred to as "*bursting*".

The recurrent collateral (CA3-CA3) synapses that provide the positive feedback that underlies burst activity in CA3 (Traub and Wong, 1982; Miles and Wong, 1983) share many properties with the closely related and well-studied Schaffer collateral synapses that connect CA3 cells to CA1 pyramidal cells (Debanne et al., 1996, 1998). Electron microscopic studies of the CA3-CA1 synapses demonstrate that there are between 2 and 36 docked glutamate vesicles per pyramidal cell synapse (Harris and Sultan, 1995; Schikorski and Stevens, 1997). Electrophysiologic studies indicate that the number of vesicles that are available for immediate release (N_R) at a synapse varies between 1 and 15 (Rosenmund and Stevens, 1996; Dobrunz and Stevens 1997; Goda and Stevens 1998; Stevens and Wesseling, 1998). When N_R is depleted it is replenished from a reserve pool (Liu and Tsien, 1995) and recycled vesicles (Darcy et al., 2006) with a time constant of 1 to 10 seconds at 36°C (Ryan and Smith, 1995; Stevens and Tsujimoto, 1995; Murthy et al., 1997). Prior work in this lab indicated exhaustion of this releasable pool of glutamate is a mechanism for burst termination (Staley et al., 1998), and the time needed for replenishment of the pool determines the minimum duration of the quiescent period between bursts (Staley et al., 2001).

Various approaches exist for designing computational models of hippocampus and other regions of the brain (Miles and Traub, 1991; Schmajuk and DiCarlo, 1992; Gluck and Myers, 1993; Maass, 1997; Hasselmo and McClelland, 1999; Dayan and Abbott, 2001; Maass, 2001; Rougier and O'Reilly 2002; Gluck et al., 2003; Lopes da Silva et al., 2003a, b; Yee et al., 2003; Abbott and Regehr, 2004; Fusi et al., 2005). Most are concerned with discovering mechanisms related to memory encoding or diseases such as Alzheimer disease (Hasselmo and McClelland 1999) and epilepsy (Lopes da Silva et al., 2003a, b; Yee et al., 2003) or to modeling certain phenomena such as glutamate release and receptor saturation (Holmes, 1995; Li and Holmes, 2000).

The goal of this work was to understand the role synaptic properties, including use-dependent synaptic depression and recovery, in the initiation and termination of spon-

*From the Neurology Department, Massachusetts General Hospital, Boston, MA, †Department of Computer Science and Engineering, ††Pediatrics Department, University of Colorado at Denver Health Sciences Center, Denver, CO.

Address correspondence and reprint requests to Dr. Kevin Staley, Neurology Department, VBK 910, Massachusetts General Hospital, 55 Fruit Street, Boston, MA 02114; e-mail: kstaley@partners.org.

ISSN: 0736-0258/07/2402-0165

taneous bursts in area CA3 of the hippocampus. We wished to develop the simplest possible neural network that would capture the essential elements of CA3 behavior and then use that network to investigate phenomena that are not amenable to pharmacologic experiments *in vitro*. We developed a model that incorporated synapses that underwent physiologically relevant depression and recovery implemented in a network of spiking neurons (NSN) model (Swiercz et al., 2006). In this article, the output of the NSN is compared with data obtained from CA3 *in vitro*, to validate the NSN and thereby permit in silico exploration of network effects of phenomena that cannot be experimentally manipulated, such as the effects of altered kinetics of synaptic depression and recovery, changes in the size of the releasable glutamate pool, and altered synaptic connectivity.

METHODS

Presynaptic Releasable Glutamate Model

We based the presynaptic elements of our model on the data of detailed physiologic experiments by Dobrunz and Stevens (1997) and Staley et al. (1998). Glutamate is released at the presynaptic terminal as a probabilistic event (Volgushev et al., 2004) where release probability is constrained by the number of vesicles containing full a quantum of glutamate, because only these vesicles are ready to release. The relation is nonlinear, but in general the higher the number of ready vesicles, the higher the release probability. Every glutamate release event decreases the probability of the release for the next arriving spike.

Glutamate replenishment is slow compared with glutamate release. The time constant for filling up an empty pool of glutamate vesicles without intervening glutamate release varies between 2 and 10 seconds (Staley et al., 1998) and possibly depends on amount of extracellular calcium (Regehr, 1997).

The amount of glutamate in a synapse depends on synapse stimulation and the rate of replenishment and is described by the following equation:

$$RG\,(t+1) = RG\,(t) - \Delta RG_{replenished}\,(t)$$

where: RG is the amount of releasable glutamate, $\Delta RG_{released}$ is the amount of glutamate released, and $\Delta RG_{replenished}$ is the amount of glutamate replenished.

When synaptic activity is low, the glutamate release is less than or equal to glutamate replenishment; thus, synaptic responses are not affected by the amount of available glutamate. However, during high rates of synaptic activity, glutamate release becomes larger than glutamate replenishment; thus, all of the release ready vesicles may become exhausted and the synapse may become temporarily inactive.

In addition to action potential-dependent glutamate release, synaptic terminals can also release glutamate spontaneously (Fatt and Katz, 1952; Kimura et al., 1997; Staley et al., 1998; Bains et al., 1999; Erickson et al., 2006). In general, the probability of spontaneous glutamate release is very low (*in vitro*) and is proportional to the size and fullness of glutamate reserve pool. The frequency of spontaneous glutamate release summed over all afferent synapses onto a CA3 neuron is approximately 1 Hz (Staley et al., 1998). This translates to a probability of 0.001 per millisecond. Because every neuron has a large amount of afferent synapses, the probability of spontaneous glutamate release for a single synapse is proportionately lower. Figure 1 shows the scheme implemented in our model. The number of releasable glutamate vesicles and the probability of their release regulate the synchronous activity of the CA3 network (Staley et al., 2001).

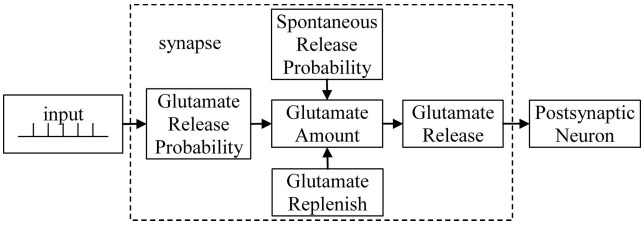

FIGURE 1. Model of glutamate release mechanism; RG–releasable glutamate.

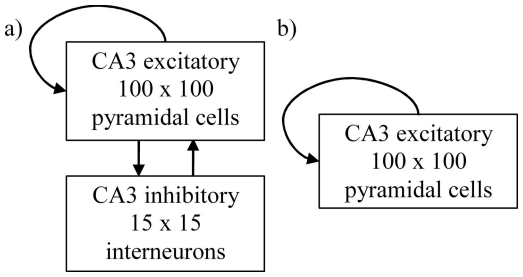

FIGURE 2. Artificial neural network model of CA3. **a)** Network including pyramidal cells and inhibitory interneurons. **b)** Network with removed interneurons.

Network Topology

Based on the hippocampus circuitry, we designed the artificial network model of a small part of hippocampus (see Fig. 2). We focus on the CA3 region because most of our experimental data were recorded in this region. Our network model accounts for both pyramidal (excitatory) and interneurons (inhibitory) cells, which play important physiologic roles in hippocampal circuitry. The dimensions of our network were 100 by 100 pyramidal neurons blended with a 15 by 15 array of interneurons. The total number of neurons was 10,225. In the majority of experiments we modeled the full network (see Fig. 2a); however, for experiments with blocked inhibition we removed the interneurons (see Fig. 2b). The ratios of neurons used within the models are based on neuroanatomical data from mice and rats (Amaral et al., 1990; Johnston and Amaral, 1998; Morin et al., 1998; Shepherd and Harris 1998; Gulyas et al., 1999; Feng et al., 2001a, b). Every neuron could connect to its neighbors within a radius of six neurons. Pyramidal cells had recurrent collateral connections and they were also connected to interneurons, whereas interneurons were connected only to pyramidal cells (see Fig. 2) (later iterations of the model will include interneuron-interneuron chemical and electrotonic junctions). The

glutamate replenishment time constant was set to 10 seconds (Staley et al., 1998). Synaptic strengths in our model are normalized namely minimum value for single connection is 0.0 and maximum value is 1.0. All synapse strengths in the network were generated randomly using Gaussian probability density. For excitatory synapses mean value was 0.5 with a standard deviation of 0.1, whereas for inhibitory synapses mean value was 0.75 with a standard deviation of 0.15.

The connections in our network are not wrapped around edges, meaning that neurons from the right side of the network are not connected to the ones on the left side of the network. The same is true for top and bottom neurons. The advantage of this design is the following: when a burst propagates outside the network via one edge it does not appear on the opposite one. This allows us to observe two-dimensional network activity. The disadvantage of our design is the edge effect: neurons close to the edges receive less synaptic input thus behave differently from the rest of neurons. To overcome this effect, we generated networks with larger dimensions and focus our measurements on the central neurons.

Neuron Model

The neuron model we used in the NSN is the improved integrate-and-fire model of MacGregor (MacGregor 1987, 1993; Gerstner, 2002), which models the physiologic neuron behavior closely in terms of subthreshold membrane potential, potassium channel response, refractory properties, neuron's excitation and inhibition, and adaptation to the stimulus.

The iteration time step for the model is 1 millisecond. In every iteration, the state of each neuron and synapse is updated depending on current state and input values.

The membrane potential is calculated based on the sum of conductances of all afferent excitatory and inhibitory synapses and of the potassium conductance. Excitatory and inhibitory conductances simulate the impact on membrane potential of the inward Na^- and Ca^- currents. Namely, excitatory conductances increase the membrane potential while inhibitory conductances decrease it. When the value of membrane potential is larger than the value of threshold neuron, an action potential is generated. Immediately after generation, a neuron is incapable of firing for a short time called the absolute refractory period. Following the absolute refractory period is an interval known as the relative refractory period, when the neuron can only fire in response to a very strong stimulation. This phenomenon is controlled in our model by the potassium conductance, simulating the outward K^+ currents. The value of the threshold in our model accommodates relative to the membrane potential value. In addition, we included membrane potential noise, representing all phenomena that may have an impact on the membrane potential and that we have not specifically implemented in our neuron model. The value of noise is calculated as a random number $\pm 5\%$ of maximum membrane potential value (mean of 0). Details are provided in Swiercz et al. (2006).

Previously, we used NSN for modeling of the somatosensory system in primates (Sala et al., 1997; Sala and Cios 1998), solving optimization problems in graphs within NSN (Sala and Cios 1999; Cios and Sala 2001), diabetic retinopathy image segmentation (Cios et al., 2004), and for edge detection in medical images (Swiercz et al., 2006). To use the NSN in modeling of physiologic experiments that target simultaneous bursts, we included the presynaptic elements described above (Dobrunz and Stevens 1997; Staley et al., 1998; Bains et al., 1999; Staley et al., 2001). Detailed descriptions of our neuron model and synaptic plasticity rules can be found in Cios et al. (2004) and Swiercz et al. (2006).

We tested different dimensions of our computational network model including a) 10 by 10, b) 25 by 25, c) 50 by 50, d) 100 by 100, and e) 300 by 300 of pyramidal cells with 5% inhibitory neurons blended in. We found that in network a the pattern of burst propagation was not visible, whereas in b and c it was it was only partially visible. Network d was large enough to observe bursts propagation patterns and there were enough neurons in the network to start recording only from part of them using our electrode model. We also ran computations for larger network e, but the computational time and memory requirements were increased and there were no advantages in the observed results. Thus, we decided that the 100 by 100 network is optimal for our computations; this size network approximates the size of the CA3 network in the slice preparation (Traub and Miles, 1991).

Recording Electrode Model and Burst Detection

To save the results of the experiments and to automatically detect network bursts, we developed a recording electrode model. The electrode was placed in the center of the network area and recorded membrane potentials and spikes of neurons located within a radius of 32 cell bodies from the electrode position at the center of the network. The strength of the recorded signal decreased with distance from the electrode. We used a Gaussian function shape for this purpose. The use of the electrode model resulted in bursts-length measurements similar to those recorded *in vitro* (Staley et al., 1998).

RESULTS

Modeling Burst Initiation.

Spontaneous bursting in the CA3 region can be induced physiologically by increasing the extracellular potassium from 2.5 to 8 mmol/L (Korn et al., 1987). This causes an increase in neurons' membrane potential (Bains et al., 1999); thus, neurons require less excitatory input for action potential generation. In the NSN model, we achieve the same result by decreasing the difference between action potential threshold and the resting membrane potential; this difference is abbreviated ΔTh_0. This led to periodic synchronous bursts of network activity (see Fig. 3). Bursting causes increased excitation of all neurons. During this activity, the supply of releasable glutamate is quickly depleted, causing burst termination.

We simulated physiologic experiments measuring interburst intervals (IBI) and burst lengths vs. extracellular potassium level. Gradual changes of extracellular potassium from 4.5 through 10.5 mmol/L caused mean IBI to decrease from 20 seconds to below 1 second (Staley et al., 2001); see Fig. 4.

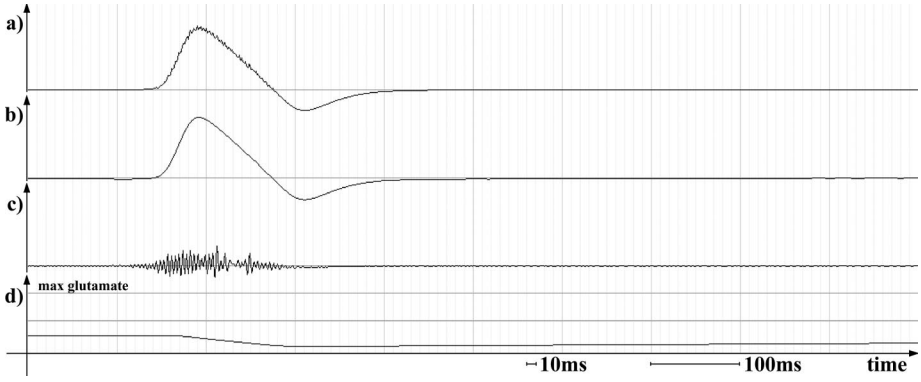

FIGURE 3. Example of 1-second network activity with occurrence of a spontaneous burst: **a)** membrane potential, **b)** filtered low-pass (1–100 Hz), **c)** filtered high-pass (200–500 Hz), **d)** mean quantity of releasable glutamate at recurrent synaptic terminals. Network size 100 by 100 pyramidal cells and 15 by 15 inhibitory cells, $\Delta Th_0 = -2mV$, mean IBI = 4.6 seconds, filtering done with FFT Butterworth filter.

We gradually decreased the difference in action potential threshold by 5 mV from control and measured IBIs and burst durations. We observed a decrease in mean IBI from 29.5 seconds to 1.8 seconds. The results of the experiment (Table 1 and Fig. 5) were satisfactory, although the decrease in burst duration at short IBI was fairly modest compared with the *in vitro* data (Staley et al., 2001).

Additionally, the simulation demonstrates postburst afterhyperpolarizations caused by inhibitory activity that was previously considered a candidate mechanism for burst termination (Fig. 4; Staley et al., 1998, 2001).

Simulation of Bursts With Blocked Inhibition

As mentioned earlier, the afterhyperpolarization associated with calcium, voltage, and synaptically gated inhibitory inputs has an impact on burst duration. However, biologic evidence shows that burst termination is possible without inhibition (Staley et al., 1998). Additionally, physiologic experiments show a moderate increase of burst length and no significant change in IBI length when inhibition is blocked. This indicates the inhibitory mechanism is not the main factor responsible for burst termination. We blocked inhibition in our model; namely, we deleted all inhibitory connections. Then we performed the same series of simulations as in previous experiment and compared the results presented in Table 2. The results conformed closely to the electrophysiologic observations (Staley et al., 1998). Bursts were successfully terminated without synaptic inhibition, and blocking inhibition caused a moderate increase in burst length. Figure 5 shows graphs comparing the results of a normal network (♦) and a network with blocked inhibitory connections (□). Figure 6 shows an example of spontaneous burst during 1 second of network activity when inhibition is blocked. It is similar to activity of the normal network presented in Fig. 3. The difference is a lack of afterhyperpolarization that is a result of blocked inhibition.

Investigating Possibility of Burst Termination by Inhibition

One possible mechanism of burst termination is a dramatic increase of inhibitory conductances (Traub and Miles 1991; Staley et al., 1998, 2001). However, the amount of inhibition required exceeds physiologic data. Proving that glutamate depletion is sufficient for burst termination *in vitro* is difficult because the supply of releasable glutamate cannot be measured or cleanly manipulated. We designed an experiment to check this theory and to asses the approximate amount of inhibitory input increase needed to stop network bursts. We used the same network topology as in previous experiments. We fixed ΔTh_0 to be equal to $-2mV$ that for previous experiments evoked a spontaneous burst with a mean IBI of 4.6 seconds. Then we decreased the value of glutamate replenishment time constant (T_{Gl}) from 10 seconds to 0.01 milliseconds to simulate a hypothetical situation in which the supply of releasable glutamate is infinite. In addition, we decreased glutamate release probability by 10% so it was not 99% all the time. As expected, network reaction was an infinite burst (Fig. 7a). Next, we began to increase the strength of inhibitory inputs. Table 3 presents the results of this experiment. In cases where bursts were not terminated, burst length was marked with "∞" and IBI "−"; otherwise, the table shows burst lengths in milliseconds and IBI in seconds. Very strong inhibition, far beyond physiologic conditions (Staley et al., 1998, 2001), can terminate bursting

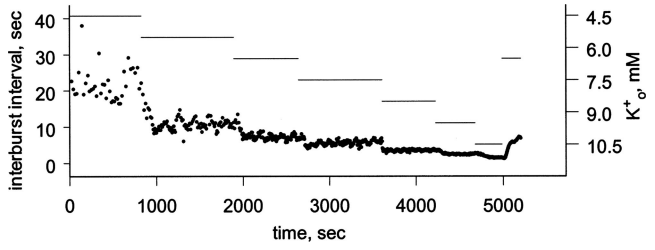

FIGURE 4. Effect of interburst interval dependency on extracellular potassium (K_o^+) level (reproduced with permission from Staley et al., 2001).

TABLE 1. Mean IBI and Burst Length Dependency on Membrane Threshold ΔTh_0 Level

ΔTh_0 vs. Control Value [mV]	0	−1	−2	−3	−4	−5
K_o^+ level approximation [mM]	2.5	5.0	6.0	7.5	9.0	10.5
Mean IBI [s]	29.5	10.2	4.6	3.0	2.2	1.8
Mean burst length [ms]	192	177	176	178	170	176
Mean burst frequency [Hz]	0.01	0.04	0.10	0.16	0.20	0.25

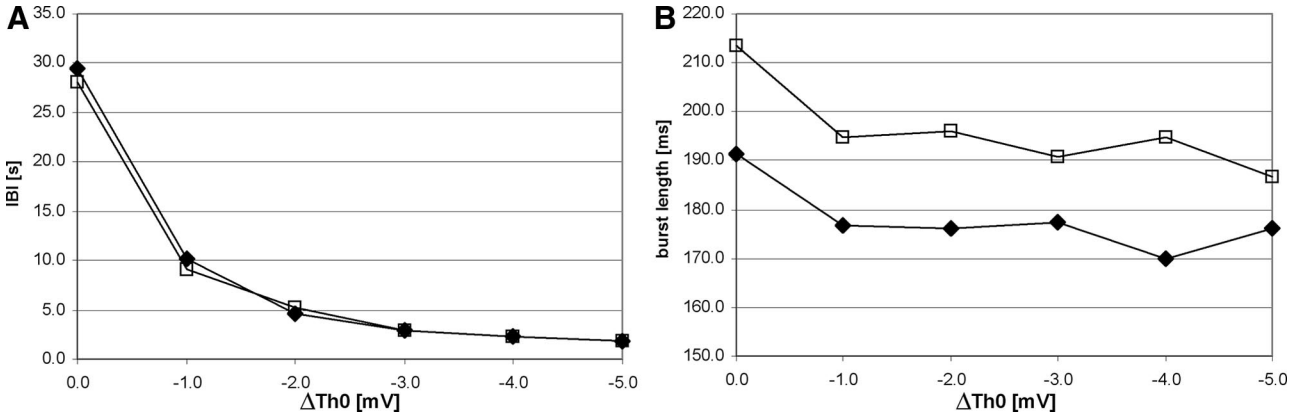

FIGURE 5. Effect of inhibition on interburst interval **(a)** and burst length **(b)**. Results compare networks with (♦) and without (□) inhibition.

(Fig. 7b). However, even this strong inhibition does not result in normal mean IBI of 4.6 seconds. Our experiment indicates that inhibitory input is capable of terminating bursts, but an extreme amount of inhibition is required. This confirms physiologic evidence that the postburst afterhyperpolarization associated with inhibitory input is not the main mechanism for burst termination.

Glutamate Release Probability Impact on Interburst Interval and Burst Length

In physiologic experiments, changing the probability of glutamate release at recurrent collateral synapses has a strong effect on burst probability (Staley et al., 1998). We therefore investigated the influence of the glutamate release probability on IBI and burst length. The threshold value (ΔTh_0) was set to −2 mV from control. Under baseline conditions, the mean IBI value was 4.6 seconds and the mean burst length was 176 milliseconds. Changing the glutamate release probability to −40%, −20%, +20%, or +40% of the original value led to corresponding changes in IBI and burst length (Table 4). Decreasing the release probability caused an increase of both mean IBI and burst length, whereas increasing release probability had the opposite effect (Table 4 and Fig. 8). The results agree with physiologic evidence from Staley et al. (2001).

Impact of Synaptic Strength on Interburst Interval and Burst Length

Synchronous activation of presynaptic and postsynaptic elements induces long-term increases in synaptic strength (Dan and Poo, 2006). This condition is satisfied during CA3 population bursts, leading to long-term increases in the strength of recurrent collateral synapses (Bains et al., 1999; Behrens et al., 2005). Long-term synaptic plasticity is calcium dependent, and lesser calcium influx leads to long-term depression of synaptic strength (Lisman, 1989; Nishiyama et al., 2000). When calcium influx via NMDA receptors is partially blocked during CA3 bursts, the recurrent collateral synapses undergo LTD (Bains et al., 1999) with consequent decreases in burst probability (Staley et al., 2001). We investigated whether our model network would accurately reflect the impact of long-term potentiation (LTP) and long-term depression (LTD) on network bursting behavior. To normalize the level of synaptic strength in the network, we first calculated the maximum possible synaptic strength as a count of all excitatory connections within the network (because maximum value for single connection was 1.0). To calculate the current mean level of synaptic strength, we calculated the sum of all excitatory connections strengths (ranging from 0.0 to 1.0) and divided the result by the maximum possible

TABLE 2. Impact of Blocking Inhibition on Mean Interburst Interval and Burst Length

ΔTh_0 vs. Control [mV]	0	−1	−2	−3	−4	−5
IBI						
Normal network [s]	29.5	10.2	4.6	3.0	2.2	1.8
Blocked inhibition [s]	28.1	9.1	5.3	3.0	2.3	1.9
Burst length						
Normal network [ms]	191	177	176	178	170	176
Blocked inhibition [ms]	213	195	196	191	195	187
Frequency						
Normal network [Hz]	0.010	0.043	0.103	0.157	0.203	0.246
Blocked inhibition [Hz]	0.010	0.046	0.087	0.153	0.203	0.240

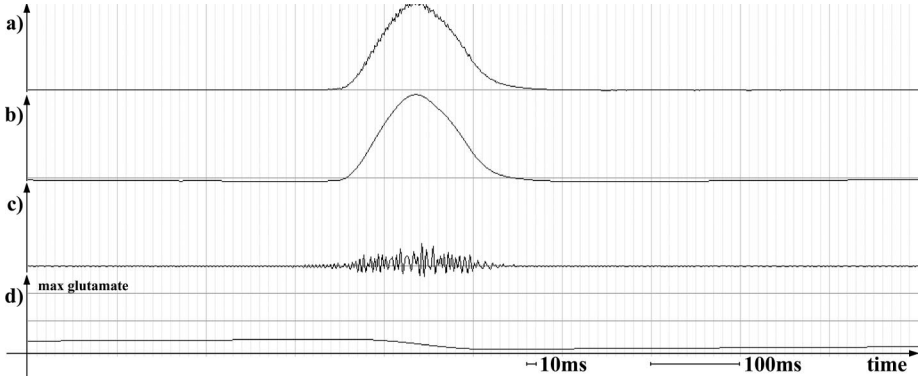

FIGURE 6. Example of 1-second network activity with disabled inhibition: **a)** membrane potential, **b)** filtered low-pass (1–100 Hz), **c)** filtered high-pass (200–500 Hz), **d)** releasable glutamate level. Network size 100 by 100 pyramidal cells and 15 by 15 inhibitory cells, $\Delta Th_0 = -2mV$, mean IBI = 5.3 seconds, filtering done with FFT Butterworth filter.

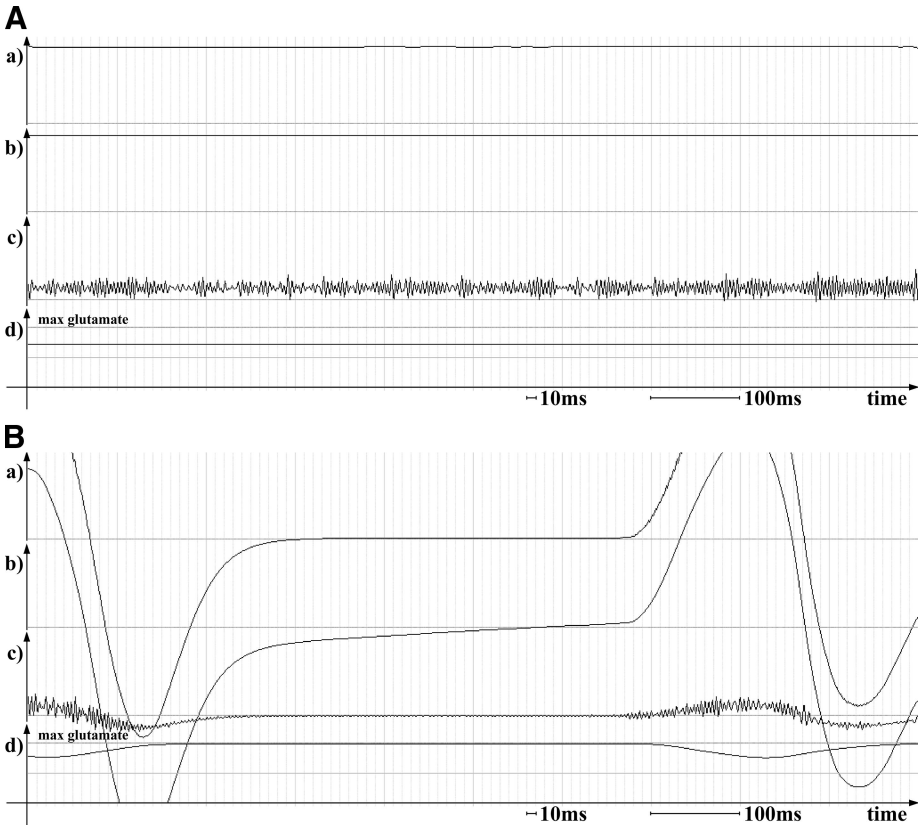

FIGURE 7. Network activity with infinite amount of releasable glutamate: A) normal inhibition $E_i = 10$ mV (IPSP reversal potential 10 mV negative to RMP) bursts were not stopped; B) extremely strong inhibition $E_i = 70mV$ (IPSP reversal potential 70 mV negative to RMP), IBI = 1.06s. **a)** Membrane potential, **b)** filtered low-pass (1–100 Hz), c) filtered high-pass (200–500 Hz), **d)** releasable glutamate level. Network size 100 by 100 pyramidal cells and 15 by 15 inhibitory cells, $\Delta Th_0 = -2mV$, filtering done with FFT Butterworth filter.

TABLE 3. Interburst Interval Values Depending on T_{GI} and E_i Settings

	T_{GI} = 0.01 ms		
E_i [mV]	Length [ms]	IBI [s]	Terminated
10	∞	—	No
40	∞	—	No
55	∞	—	No
62	270.6	1.09	Yes
70	213.7	1.06	Yes

TABLE 4. Changes in IBI and Burst Length Caused by Release Probability Changes

Release Probability Rate Change	−40%	−20%	0%	+20%	+40%
Mean IBI [s]	11.2	6.4	4.6	3.8	3.0
Mean burst length [ms]	194	181	176	173	167

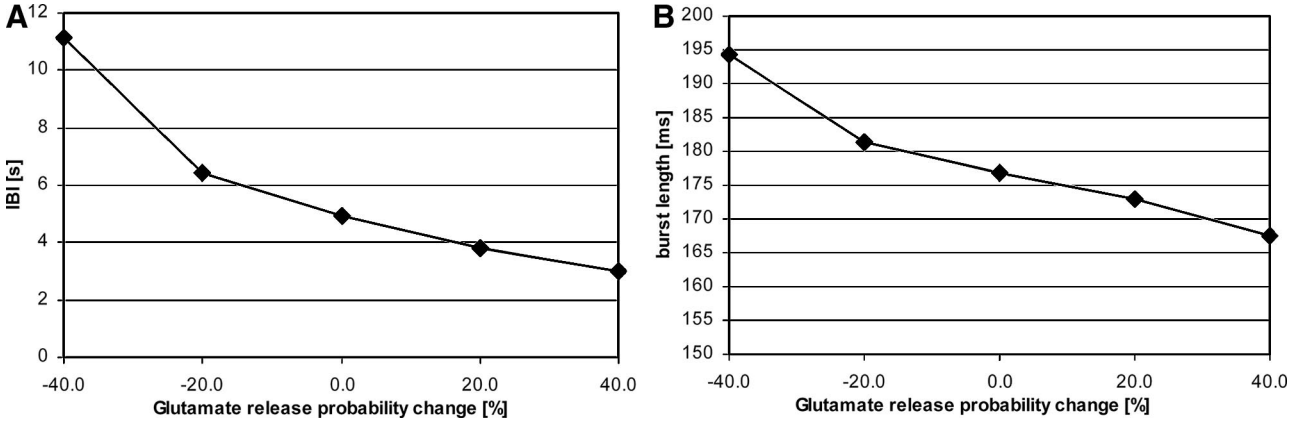

FIGURE 8. Relationship between glutamate release probability and **a)** IBI and **b)** burst length.

potentiation. To get the percentage value, we then multiplied it by 100%. We set specific values of mean network synaptic strengths, ranging between 30% (LTD) and 95% (LTP) of maximum, and simulated 15 minutes of network activity. For every simulation, we randomly generated new synaptic strength values for all excitatory connections, picking new synaptic strength values from the range ±15% from the mean network synaptic strength using Gaussian probability density. For every randomly generated network mean synaptic strength, we measured IBI and mean burst length (Table 5, Fig. 9).

The results demonstrate a nonlinear relationship between the network average level of synaptic strength versus IBI and burst length. There is a rapid increase in mean IBI between mean values of synaptic strength of 50% and 55%. For the connection strengths close to 95%, the network is almost constantly bursting in a way similar to the ictal-sustained state described in Dzhala and Staley (2003). However, for average network synaptic strengths below 45% (long-term depression), our network did not burst at all during the experiment. The average burst length was not affected by network potentiation in a range from 50% to 90%. For the network potentiation of 45%, there was small increase of burst length; however, it may be caused by the fact that the average was based on only two bursts.

Our results show that LTP and LTD can strongly affect the network bursting behavior, and are consistent with electrophysiologic experiments (Bains et al., 1999; Behrens et al., 2005; Staley et al., 2001). At network potentiation below 45%, bursting stopped. This is consistent with the results of simulations using much more elaborate models of postsynaptic neurons (Traub and Miles, 1991) and the results of electrophysiologic experiments (Bains et al., 1999).

OBSERVATION OF LTP

The prior results demonstrate that changes in synaptic strength are sufficient to alter the temporal pattern of network bursting. The reverse has also been demonstrated: network burst activity is sufficient to induce long-term changes in synaptic strength (Bains et al., 1999; Behrens et al., 2005). In the following computational experiments, we simulated the physiologic experiment by Bains et al. (1999) in which they observed a 100% increase in synaptic strength following 15 to 30 minutes of spontaneous network bursting. The bursting was induced *in vitro* by a transient increase in extracellular K_o^+, and in the simulation by decreasing the difference between membrane potential and action potential threshold and increasing the probability of glutamate release (Fig. 4). The increase in synaptic strength observed by Bains et al. (1999) was specific to CA3-CA3 recurrent collateral synapses, demonstrating that it was the result of synchronized bursting and not the transiently increased K^+ level.

We used a model of spike timing dependent induction of synaptic plasticity (Dan and Poo, 2006) as previously described (Swiercz et al., 2006). Because of computational time limitations we were not able to perform a 30-minute experiment on our network model. Thus, we decreased the length of simulation to 5 minutes. To compensate for shorter time, we increased the rate of network bursting by setting ΔTh0 to -5 mV from control, resulting in IBI of 1.8 seconds. We also increased synaptic plasticity in the network by tripling the learning rate. Synchronous network activity increased the strength of recurrent collateral CA3 synapses by 40%. Although the amount of the increase was not the same as in the physiologic experiment, the trend of potentiation

TABLE 5. Relationship Among Network Potentiation, IBI, and Burst Length

Potentiation Ratio [%]	45	50	55	60	65	70	90
Mean IBI [s]	42.6	12.7	5.0	3.0	2.3	2.0	1.4
Burst length [ms]	194.0	177.0	176.8	174.2	177.5	176.6	174.6

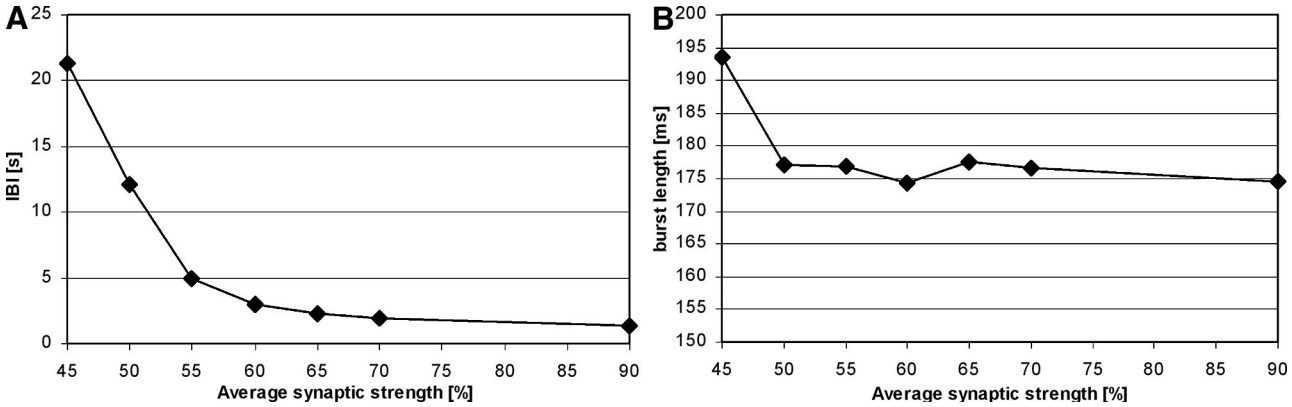

FIGURE 9. Relationship between average strength of recurrent collateral synapses and **a)** IBI and **b)** burst length.

change was the same, and the increase in strength is well within the range of experimentally induced LTP.

OBSERVATION OF TWO-DIMENSIONAL BURST IN THE CA3 REGION OF HIPPOCAMPUS

Our network model allows observation of two-dimensional aspects of network behavior. This can help to investigate not only the frequency of bursts but also their origin. We can show the two-dimensional image of network activity, the local supply of available glutamate, and synaptic strength. Thus, we can investigate if a particular burst origin region was correlated with certain glutamate accumulation and/or local synaptic strength increase, or if the anatomic source of the burst is random. By analyzing two-dimensional bursting activities, we discovered that for randomly generated synaptic strengths, there were no specific regions responsible for bursts initiation. There was no indication for higher glutamate accumulation or higher synaptic strength in regions of burst initiation. However, sometimes connections within a particular region were a bit stronger than the average, which caused minor increase of burst initiation probability in this region but did not prevent other regions from initiating bursts. Figure 10 shows an example of two-dimensional burst activities.

DISCUSSION

We have developed a computational model of neuronal circuits of the CA3 hippocampal region incorporating simple integrate and fire neurons whose synaptic connections included use-dependent depression and recovery from depression. This model reproduced key experimental findings including periodic self-limited population bursts, the effects of reduced glutamate release probability, the effect of membrane depolarization, and the effects of long-term changes in average synaptic strength. These results indicate that synaptic depression and recovery play a very important role in initiation and termination of periodic synchronous network activity, and support the use of this model in the investigation of phenomena that are not easily addressed experimentally.

The postsynaptic elements of this model were purposefully kept simple. A network with realistic presynaptic elements and simple postsynaptic elements that captures the key features of multiple physiologic experiments supports the hypothesis that the key determinants of burst initiation and termination are presynaptic. It should be noted that the converse has also been demonstrated: that is, a model with sophisticated postsynaptic elements and purposefully simple presynaptic elements also reproduces burst initiation and termination (Traub and Miles, 1991). For this reason we

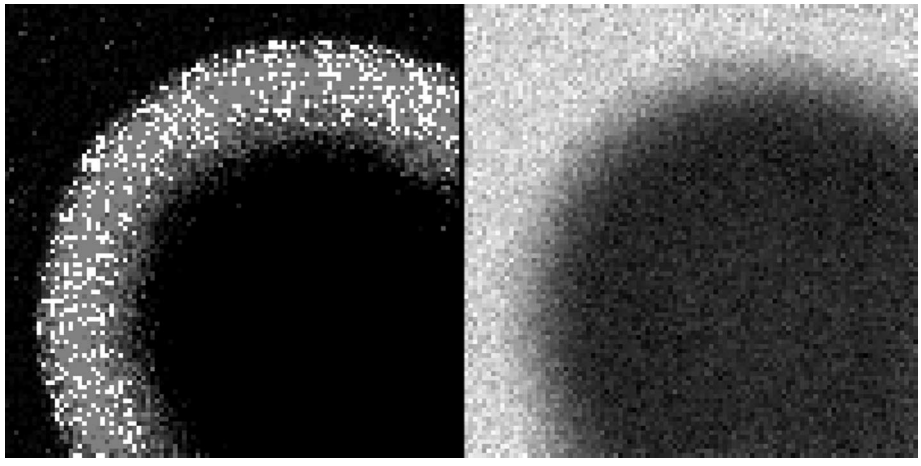

FIGURE 10. Two-dimensional burst propagation. Left image shows the potentials and the right image shows the glutamate level.

tested the current "presynaptic" model under a variety of experimental conditions and explicitly studied the effects of inhibitory conductances as a burst termination mechanism.

We performed a number of physiologically inspired experiments. First, we investigated various aspects of bursts initiation and termination and the role of inhibition in this process. We observed the influence of LTP and LTD on the bursting activity, and the influence of the bursts on the LTP. The results of all experiments agreed with physiologic experiments; thus, we consider our model development a success. Additionally, we investigated the possibility of burst termination by inhibitory inputs. We found that the amount of inhibition required to stop the burst exceeds what has been observed physiologically (Staley et al., 1998, 2001).

Our findings show that we can control bursting activity by altering several important parameters of the network. The most important one is releasable glutamate availability. By decreasing the amount of available releasable glutamate, we influence the only way the bursts can develop and propagate. This can be achieved by slowing down glutamate replenishment, decreasing glutamate release rate, and decreasing the maximum amount of glutamate available. Another parameter allowing control of the network bursting activity is neuron excitation. One can decrease the neurons' excitation to slow down its firing rate, thus affecting spontaneous bursts frequency. Because neurons' excitation is related to synaptic potentiation, we modeled an important phenomenon that may be crucial for controlling spontaneous bursting. Namely, we showed that bursting induces LTP, which in turn increases burst probability. By preventing the LTP, we could interrupt this self-feeding loop. We have shown in our experiments that there is a synaptic strength potentiation level below which bursts are strongly impaired or disabled (Traub and Miles, 1991). This supports the idea of impairing bursting activity by causing strong LTD of the synapses that comprise the positive feedback elements in a network. Because LTD is not easily reversed, it may prove to exert a long-term effect on bursting activity and thus could be a possible substitute for surgical procedure in case of severe epilepsy (Bains et al., 1999).

Our model makes feasible the observation of network activity in two dimensions. This is important for analyzing spatial factors influencing bursting such as the speed of burst propagation and afterbursts. In the two-dimensional studies of burst initiation and propagation, we did not find any specific regions that were consistently responsible for bursts initiation. This is consistent with statistical data that do not support a single burst initiation site (Staley et al., 2001). Using stochastic distribution of initial synaptic strengths, we never observed a region that consistently initiated a burst, although that might be possible with sufficiently broad distribution of synaptic strengths. However, we have noticed that regions with increased synaptic strengths were initiating bursts more often than other areas.

By analyzing two-dimensional network activity, we were also able to point out the importance of increasing simulated network models size. In our experiments, small network size reduced the reliability of experiments results. Our findings show that the network dimensions 100 by 100 cells are sufficient when network edges are not randomly connected back into the network.

This artificial network of spiking neurons model is a tool that is validated and can now be successfully applied for physiologically inspired but pharmacologically infeasible experiments. The model should be helpful in further understanding of physiologic data or investigating theories that are difficult to study in physiologic experiments.

ACKNOWLEDGMENTS

This work was supported by NIH grants NS040109, NS 034360, and NS 034700.

REFERENCES

Abbott LF, Regehr WG. Synaptic computation. *Nature.* 2004;431:796–803.
Amaral DG, Ishizuka N, Claiborne B. Neurons, numbers, and the hippocampal network. *Prog Brain Res.* 1990;83:1–11.
Bains JS, Longacher JM, Staley KJ. Reciprocal interactions between CA3 network activity and strength of recurrent collateral synapses. *Nat Neurosci.* 1999;2:720–726.
Behrens CJ, van den Boom LP, de Hoz L, et al. Induction of sharp wave-ripple complexes in vitro and reorganization of hippocampal networks. *Nat Neurosci.* 2005;8:1560–1567.
Chamberlin NL, Traub RD, Dingledine R. Role of EPSPs in initiation of spontaneous synchronized burst firing in rat hippocampal neurons bathed in high potassium. *J Neurophysiol.* 1990;64:1000–1008.
Cios KJ, Sala DM. Networks of Spiking Neurons in Data Mining. In: Pal SK, Pal A, eds. *Pattern recognition: from classical to modern approaches.* New Jersey: World Scientific, 2001;329–346.
Cios KJ, Swiercz W, Jackson W. Networks of Spiking Neurons in Modeling and Problem Solving. *Neurocomputing.* 2004;61:99–119.
Dan Y, Poo MM. Spike timing-dependent plasticity: from synapse to perception [Review]. *Physiol Rev.* 2006;86:1033–1048.
Darcy KJ, Staras K, Collinson LM, Goda Y. Constitutive sharing of recycling synaptic vesicles between presynaptic boutons. *Nat Neurosci.* 2006;9:315–321.
Dayan P, Abbott LF. Theoretical neuroscience: computational and mathematical modeling of neural systems. Cambridge: MIT Press, 2001.
Debanne D, Guerineau NC, Gahwiler BH, Thompson SM. Paired-pulse facilitation and depression at unitary synapses in rat hippocampus: quantal fluctuation affects subsequent release. *J Physiol.* 1996;491:163–176.
Debanne D, Gahwiler BH, Thompson SM. Long-term synaptic plasticity between pairs of individual CA3 pyramidal cells in rat hippocampal slice cultures. *J Physiol.* 1998;507(Pt 1):237–247.
Dobrunz LE, Stevens CF. Heterogeneity of release probability, facilitation, and depletion at central synapses. *Neuron.* 1997;18:995–1008.
Dzhala VI, Staley KJ. Transition from interictal to ictal activity in limbic networks in vitro. *J Neurosci.* 2003;23:7873–7880.
Erickson JD, De Gois S, Varoqui H, et al. Activity-dependent regulation of vesicular glutamate and GABA transporters: a means to scale quantal size, *Neurochem Int.* 48:643–649, 2006.
Fatt P, Katz B. Spontaneous subthreshold activity at motor nerve endings. *J Physiol.* 1952;117:109–128.
Feng J, Brown D, Wei G, Tirozzi B. Detectable and Undetectable Input Signals For The Integrate-and-Fire Model. *J Phys A.* 2001a;34:1637–1648.
Feng J, Li GB, Brown D, Buxton H. Balance between four types of synaptic input for The Integrate-and-Fire Model. *J Theor Biol.* 2001b;203:61–79.
Fusi S, Drew PJ, Abbott LF. Cascade models of synaptically stored memories. *Neuron.* 2005;45:599–611.
Gerstner W. Integrate and Fire Neurons and Networks. In: Arbib MA, ed. *The handbook of brain theory and neural networks,* 2nd ed. Cambridge: MIT Press, 2002.
Gluck MA, Meeter M, Myers CE. Computational models of the hippocampal region: linking incremental learning and episodic memory. *Trends Cogn Sci.* 2003;7:269–276.

Gluck MA, Myers CE. Hippocampal mediation of stimulus representation: a computational theory. *Hippocampus.* 1993;3:491–516.
Gluck MA, Myers CE. *Gateway to memory. an introduction to neural network modeling of the hippocampus and learning.* Cambridge: MIT Press, 2001.
Goda Y, Stevens CF. Readily releasable pool size changes associated with long term depression. *PNAS.* 1998;95:1283–1288.
Gulyas AI, Megias M, Emri Z, Freund TF. Total number and ratio of excitatory and inhibitory synapses converging onto single interneurons of different types in the CA1 area of the rat hippocampus. *J Neurosci.* 1999;19:10082–10097.
Harris KM, Sultan P. Variation in the number, location, and size of synaptic vesicles provides an anatomical basis for the nonuniform probability of release at hippocampal CA1 synapses. *Neuropharmacology.* 1995;34: 1387–1395.
Hasselmo ME, McClelland JL. Neural models of memory. *Curr Opin Neurobiol.* 1999;9:184–188.
Hauser WA, Annegers JF, Rocca WA. Descriptive epidemiology of epilepsy: contributions of population-based studies from Rochester, Minnesota. *Mayo Clin Proc.* 1996;71:576–586.
Holmes WR. Modeling the effect of glutamate diffusion and uptake on NMDA and non- NMDA receptor saturation. *Biophys J.* 1995;69:1734–1747.
Jefferys JGR. Mechanisms and experimental models of seizure generation. *Curr Opin Neurol.* 1998;11:123.
Johnston D, Amaral DG. Hippocampus. In: Shepherd GM, ed. *Synaptic organization of the brain.*. Oxford: University Press, 1998;417–458.
Kandel ER, Schwartz JH, Jessell TM. *Principles of neural science.* New York: Elsevier, 2000.
Kimura F, Otsu Y, Tsumoto T. Presynaptically silent synapses: spontaneously active terminals without stimulus-evoked release demonstrated in cortical autapses. *J Neurophysiol.* 1997;77:2805–2815.
Korn SJ, Giacchino JL, Chamberlin NL, Dingledine R. Epileptiform burst activity induced by potassium in the hippocampus and its regulation by GABA-mediated inhibition. *J Neurophysiol.* 1987;57:325–40.
Li Y, Holmes WR. Comparison of CaMKinase II activation in a dendritic spine computed with deterministic and stochastic models of the NMDA synaptic conductance. *Neurocomputing.* 2000;32–33:1–7.
Lisman J. A mechanism for the Hebb and the anti-Hebb processes underlying learning and memory. *Proc Natl Acad Sci U S A.* 1989;86:9574–9578.
Liu G, Tsien RW. Properties of synaptic transmission at single hippocampal synaptic boutons. *Nature.* 1995;375:404–408.
Lopes da Silva FH, Blanes W, Kalitzin SN, et al. Dynamical diseases of brain systems: different routes to epileptic seizures. *IEEE Trans Biomed Eng.* 2003a;50:540–548.
Lopes da Silva FH, Blanes W, Kalitzin SN, et al. Epilepsies as dynamical diseases of brain systems: basic models of the transition between normal and epileptic activity. *Epilepsia.* 2003b;44:72–83.
Maass W. Networks of spiking neurons: the third generation of neural network models. *Neural Networks.* 1997;10:1659–1671.
Maass W. Computation with spiking neurons. In: Arbib MA, ed. *The handbook of brain theory and neural networks,* 2nd ed. Cambridge: MIT Press, 2001.
MacGregor RJ. *Neural and brain modeling.* New York: Academic Press, 1987.
MacGregor RJ. *Theoretical mechanics of biological neural networks.* New York: Academic Press, 1993.
Mayr O. *The origins of feedback control.* Cambridge: MIT Press, 1970.
McIntosh AM, Kalnins RM, Mitchell LA, Berkovic SF. Early seizures after temporal lobectomy predict subsequent seizure recurrence. *Ann Neurol.* 2005;57:283–288.
Miles R, Wong RKS. Single neurones can initiate synchronized population discharge in the hippocampus. *Nature.* 1983;306:371–373.
Morin F, Clermont-Beaulieu C, Lacaille JC. Selective loss of GABA neurons in area CA1 of the rat hippocampus after intraventricular kainate. *Epilepsy Res.* 1998;32:363–369.
Murthy VN, Sejnowski TJ, Stevens CF. Heterogenous release properties of visualized individual hippocampal synapses. *Neuron.* 1997;18:599–612.
Nishiyama M, Hong K, Mikoshiba K, et al. Calcium stores regulate the polarity and input specificity of synaptic modification. *Nature.* 2000; 408:584–8.
Regehr WG. Interplay between sodium and calcium dynamics in granule cell presynaptic terminals. *Biophys J.* 1997;73:2476–2488.
Rosenmund C, Stevens CF. Definition of the readily releasable pool of vesicles at hippocampal synapses. *Neuron.* 1996;16:1197–1207.
Rougier NP, O'Reilly RC. Learning representations in a gated prefrontal cortex model of dynamic task switching. *Cogn Sci.* 2002;26:503–520.
Ryan TA, Smith SJ. Vesicle pool mobilization during action potential firing at hippocampal synapses. *Neuron.* 1995;14:983–989.
Sala DM, Cios KJ, Wall JT. A spatio-temporal computer model of dynamic organization properties of the adult primate somatosensory system. In: *Proceedings of 1997 International Conference on Neural Information Processing and Intelligent Information Systems.*. Dunedin, New Zealand: Springer, 1997;153–156.
Sala DM, Cios KJ. Self-organization in networks of spiking neurons. *Aust J Intel Inform Process Syst.* 1998;5:161–170.
Sala DM, Cios KJ. Solving graph algorithms with networks of spiking neurons. *IEEE Trans Neural Networks.* 1999;10:953–957.
Schikorski T, Stevens CF. Quantitative ultrastructural analysis of hippocampal excitatory synapses. *J Neurosci.* 1997;17:5858–5867.
Schmajuk N, DiCarlo J. Stimulus configuration, classical conditioning and hippocampal function. *Psychol Rev.* 1992;99:268–305.
Shepherd GM, Harris KM. Three-dimensional structure and composition of CA3-CA1 axons in rat hippocampal slices: implications for presynaptic connectivity and compartmentalization. *J Neurosci.* 1998;18:8300–8310.
Staley K, Longacher JM, Bains JS, Yee A. Presynaptic Modulation of CA3 Network Activity. *Nat Neurosci.* 1998;1:201–209.
Staley K, Bains JS, Yee A, et al. Statistical model relating CA3 burst probability to recovery from burst-induced depression at recurrent collateral synapses. *J Neurophysiol.* 2001;86:2736–2747.
Stevens CF, Wesseling JF. Activity-dependent modulation of the rate at which synaptic vesicles become available to undergo exocytosis. *Neuron.* 1998;21:415–424.
Stevens CF, Tsujimoto T. Estimates for the pool size of releasable quanta at a single central synapse and for the time required to fill the pool. *PNAS.* 1995;92:846–849.
Swiercz W, Cios K, Staley K, et al. A New Synaptic Plasticity Rule for Networks of Spiking Neurons. *IEEE Trans Neural Networks.* 2006;17: 94–105.
Traub RD, Miles R. *Neuronal networks of the hippocampus.* Cambridge: Cambridge University Press, 1991.
Traub RD, Miles R. Collective behaviors of the CA3 network: experiment and model. In: *Neuronal networks of the hippocampus.* Cambridge: Cambridge University Press, 1991.
Traub RD, Wong RKS. Cellular mechanism of neuronal synchronization in epilepsy. *Science.* 1982;216:745–747.
Tsodyks M, Uziel A, Markram H. Synchrony generation in recurrent networks with frequency-dependent synapses. *J Neurosci.* 2000;20:1–5
Volgushev M, Kudryashov I, Chistiakova M, et al. Probability of transmitter release at neocortical synapses at different temperatures. *J Neurophysiol.* 2004;92:212–220.
Yee AS, Longacher JM, Staley KJ. Convulsant and anticonvulsant effects on spontaneous CA3 population bursts. *J Neurophysiol.* 2003;89: 427–441.